Intrinsic temperature sensitivity of tilted fiber Bragg grating based surface plasmon resonance sensors

Li-Yang Shao,[1,2,*] Yanina Shevchenko,[1] and Jacques Albert[1]

[1] *Department of Electronics, Carleton University, 1125 Colonel By Drive, Ottawa, Ontario K1S 5B6, Canada*
[2] *Institute of Optoelectronic Technology, China Jiliang University, Hangzhou 310018, China*
**liyangshao@gmail.com*

Abstract: A miniature surface plasmon resonance sensor is fabricated from a gold-coated standard optical fiber with an in-core tilted fiber Bragg grating fabricated by UV exposure. The sensor has a measured refractive index sensitivity of 571.5 nm/RIU (refractive index unit) at constant temperature. We show here that the intrinsic temperature sensitivity of this device is reduced to less than 6.3 pm/°C (between 23 °C and 59 °C) when measurements are referenced to a core mode reflection resonance of the grating. This residual sensitivity is essentially that of the 50 nm thick deposited gold layer but it is bigger by one order of magnitude than the expected value (0.51 pm/°C) for a gold-water interface.

OCIS codes: (240.6680) Surface plasmons; (280.1415) Biological sensing and sensors; (060.2370) Fiber optics sensors; (060.3735) Fiber Bragg gratings.

References and links

1. K. Matsubara, S. Kawata, and S. Minami, "Optical chemical sensor based on surface plasmon measurement," Appl. Opt. **27**(6), 1160–1163 (1988).
2. R. C. Jorgenson, and S. S. Yee, "A fiber-optic chemical sensor based on surface plasmon resonance," Sens. Actuators B Chem. **12**(3), 213–220 (1993).
3. R. Slavík, J. Homola, J. Tyroký, and E. Brynda, "Novel spectral fiber optic sensor based on surface plasmon resonance," Sens. Actuators B Chem. **74**(1–3), 106–111 (2001).
4. J. L. Tang, S. F. Cheng, W. T. Hsu, T. Y. Chiang, and L. K. Chau, "Fiber-optic biochemical sensing with a colloidal gold-modified long period fiber grating," Sens. Actuators B Chem. **119**(1), 105–109 (2006).
5. J. Pollet, F. Delport, K. P. F. Janssen, K. Jans, G. Maes, H. Pfeiffer, M. Wevers, and J. Lammertyn, "Fiber optic SPR biosensing of DNA hybridization and DNA-protein interactions," Biosens. Bioelectron. **25**(4), 864–869 (2009).
6. B. Spacková, and J. Homola, "Theoretical analysis of a fiber optic surface plasmon resonance sensor utilizing a Bragg grating," Opt. Express **17**(25), 23254–23264 (2009), http://www.opticsinfobase.org/abstract.cfm?URI=oe-17-25-23254.
7. Y. Y. Shevchenko, and J. Albert, "Plasmon resonances in gold-coated tilted fiber Bragg gratings," Opt. Lett. **32**(3), 211–213 (2007).
8. Y. Y. Shevchenko, D. A. D. Blair, M. C. Derosa, and J. Albert, "DNA Target Detection Using Gold-coated Tilted Fiber Bragg Gratings in Aqueous Media," CLEO/QELS 2008, San Jose, CA, CMJ4 (2008).
9. T. Allsop, R. Neal, S. Rehman, D. J. Webb, D. Mapps, and I. Bennion, "Generation of infrared surface plasmon resonances with high refractive index sensitivity utilizing tilted fiber Bragg gratings," Appl. Opt. **46**(22), 5456–5460 (2007).
10. S. M. Tripathi, A. Kumar, E. Marin, and J.-P. Meunier, ""Side-Polished Optical Fiber Grating-Based Refractive Index Sensors Utilizing the Pure Surface Plasmon Polariton," IEEE/OSA," J. Lightwave Technol. **26**(13), 1980–1985 (2008).
11. G. Nemova, and R. Kashyap, "Fiber-Bragg-grating-assisted surface plasmon-polariton sensor," Opt. Lett. **31**(14), 2118–2120 (2006).
12. Y. Shevchenko, C. Chen, M. A. Dakka, and J. Albert, "Polarization-selective grating excitation of plasmons in cylindrical optical fibers," Opt. Lett. **35**(5), 637–639 (2010).
13. C. F. Chan, C. Chen, A. Jafari, A. Laronche, D. J. Thomson, and J. Albert, "Optical fiber refractometer using narrowband cladding-mode resonance shifts," Appl. Opt. **46**(7), 1142–1149 (2007).
14. H.-P. Chiang, Y.-C. Wang, and P. T. Leung, "Effect of temperature on the incident angle-dependence of the sensitivity for surface plasmon resonance spectroscopy," Thin Solid Films **425**(1–2), 135–138 (2003).
15. K. Lin, Y. Lu, Z. Luo, R. Zheng, P. Wang, and H. Ming, "Numerical and experimental investigation of temperature effects on the surface plasmon resonance sensor," Chin. Opt. Lett. **7**(5), 428–431 (2009).

#126816 - $15.00 USD Received 12 Apr 2010; revised 4 May 2010; accepted 4 May 2010; published 14 May 2010

16. S. K. Ozdemir, and G. Turhan-Sayan, ""Temperature effects on surface plasmon resonance: design considerations for an optical temperature sensor," IEEE/OSA," J. Lightwave Technol. **21**(3), 805–814 (2003).
17. C. K. Chen, A. Laronche, G. Bouwmans, L. Bigot, Y. Quiquempois, and J. Albert, "Sensitivity of photonic crystal fiber modes to temperature, strain and external refractive index," Opt. Express **16**(13), 9645–9653 (2008), http://www.opticsinfobase.org/oe/abstract.cfm?URI=oe-16-13-9645.
18. The International Association for the Properties of Water and Steam, "Release on the refractive index of ordinary water substance as a function of wavelength, temperature and pressure," IAPWS, Erlangen, pp.2 (1997).
19. W.-J. Lee, J.-E. Kim, H. Y. Park, S. Park, M.-S. Kim, J. T. Kim, and J. J. Ju, "Optical constants of evaporated gold films measured by surface plasmon resonance at telecommunication wavelengths," J. Appl. Phys. **103**(7), 073713 (2008).

1. Introduction

Surface plasmon resonance (SPR) sensors have been widely used in refractive-index related measurements, including label-free bio-chemical sensing, because of their high sensitivity and real-time detection capability. Most SPR sensors are fabricated using variants of the original Kretschmann-Raether geometry [1], a bulk optics approach that uses a high index glass prism with a thin metal coating deposited on its base, and tunneling across the metal from a wave totally internally reflected inside the prism to excite the plasmon waves. In this case, plasmon resonances are found by measuring a dip in the reflection spectrum off the base of the prism, corresponding to rays that are phase matched to the plasmon (or equivalently for the angular dependence of the reflection of monochromatic light). However it was recognized early on that waveguiding of light confined in optical fibers (also by total internal reflection) could be used to implement a fiber optic equivalent of the prism geometry, with obvious advantages in terms of size and light handling properties. In 1993, Jorgensen and Yee demonstrated the first such fiber-based SPR sensor within a multimode optical fiber with its cladding removed and replaced by the metal coating in the sensing region [2]. For the fiber case, the plasmon resonance is also identified by a dip in the transmission spectrum of the guided light. This configuration became a standard for the best fiber optic SPR sensors and is still used today [3–12]. In our work on fiber SPR, we use a slightly different approach that is based on the controlled excitation of the cladding modes of a "single-mode" fiber by a tilted Bragg grating photo-inscribed in the fiber core [7,8]. In contrast to prior experimental [9,10] or proposed [11] grating-assisted fiber SPR sensors, our approach does not require custom-made fiber geometries (by design or post-fabrication modifications such as side-polishing or etching). Furthermore, we recently demonstrated that by lining up the polarization of the light launched in the fiber with the tilt plane of the grating we can excite only those cladding modes that have proper polarization (radial) to couple to plasmon modes of the outer surface of the metal coated cylindrical cladding [12]. One advantage of the single mode fiber approach (over the traditional multimode fiber implementations) lies in the fact that the spectral distribution of the guided light into the large set of cladding modes is fully determined by the well known (single) core mode properties and those of the grating used. In a multimode fiber SPR, a mode scrambler is required to try to achieve a consistent distribution of the light amongst all the modes. Another advantage of the grating-assisted single mode configuration is the possibility to deal with the thermal cross-sensitivity of the resonances. In principle, all the fiber SPR sensors suffer from the same predicament as their bulk optic equivalents, the cross-sensitivity to temperature. This effect represents a major issue for high sensitivity applications and is dealt with by complex temperature stabilization schemes in commercial instruments. In the work reported here, the temperature sensitivity of our recently developed tilted fiber Bragg grating SPR sensor is studied in detail and shown to be reducible to a few pm per degree Celcius.

It turns out that similarly to the simple tilted fiber Bragg grating (TFBG) refractometer [13], all the cladding mode resonances of the TFBG-SPR have the same temperature dependence as that of the core mode back reflection resonance (the "Bragg" resonance). Therefore the temperature sensitivity of the spectral locations of the resonances can be eliminated by referencing all wavelengths to the wavelength of the "Bragg" resonance, which by definition is otherwise impervious to changes occurring outside of the fiber cladding. Unlike the TFBG refractometer however, the TFBG-SPR sensor also includes a metal layer

#126816 - $15.00 USD Received 12 Apr 2010; revised 4 May 2010; accepted 4 May 2010; published 14 May 2010

on the fiber and its properties (including its thermal properties) are as critical as those of the outer medium in determining the SPR wavelength [1]. As the temperature changes the permittivity of the metal layer will change as well and cause an unwanted SPR shift overlaid on the shift due to the refractive index change of the outer medium (that we want to measure). While there are many papers dedicated to the understanding and calibration of the effect of temperature on SPR sensors (for both prism- and fiber-based devices) [14–16], we present here for the first time an experimental measurement of the effect of the thermal properties of the metal coating itself on the temperature sensitivity of a fiber optic SPR sensor.

2. Materials and methods

It is known that many applications of SPR in biomedical or chemical applications require measurements in aqueous solutions, so we chose distilled water as the medium in which to carry out our experiments and temperatures typical of laboratory and *in vivo* environments (23 °C to 59 °C). The experimental wavelength response of the SPR has been characterized in detail for this range of values and analyzed to extract the desired information.

The device itself was fabricated using the techniques described in reference 12: A 10 mm long fiber Bragg grating with a tilt angle of 10 degree was fabricated in a hydrogen-loaded single-mode fiber by using a phase mask and 248 nm pulsed irradiation from a KrF excimer laser. A gold coating with a thickness of 50 nm was deposited by sputtering on the surface of fabricated TFBGs, proceeding in two steps to cover the full circumference of the fiber. Figure 1 shows the schematic diagram of the TFBG SPR sensor. The grating couples the core mode to a multitude of cladding modes (each at a different wavelength, as determined by the grating period and mode effective index), and these couplings show up as loss peaks in the transmission spectrum. Because the metal layer is so thin, some of the light guided by the cladding tunnels across to the outside surface of the metal and when this light is phase matched (and has the correct polarization state) with a possible plasmon mode of the interface between the gold and the outer medium, such plasmon wave can be excited efficiently. The phase matching condition is relatively narrowband and involves only a small subset of cladding modes. When this occurs, the resonance becomes lossy and disappears from the transmission spectrum [12]: It is the position of the missing resonances that reveals the wavelength of SPR.

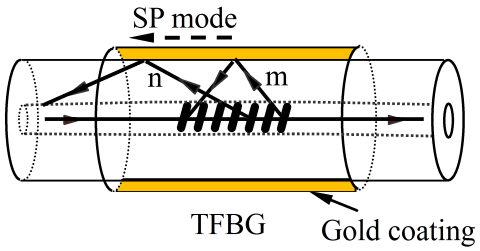

Fig. 1. Schematic diagram of the TFBG-SPR sensor.

The experimental setup for the temperature characterization is shown schematically in Fig. 2. The light from a fiber coupled broadband source (BBS: C + L band ASE source from JDSU Corporation) goes through a polarizer followed by a polarization controller used to adjust the polarization of the light reaching the TFBG. Then the transmission spectrum of the TFBG SPR sensor is measured by an optical spectrum analyzer (AQ6317B from Ando). In practice, the polarization state is simply rotated by a rotatable linear polarizer until the SPR signature is maximized (p-polarized): this corresponds to the complete extinction of a small subset of cladding mode resonances, as shown in Fig. 3. For the s-polarized light, the SPR effect cannot be excited so that the spectrum is similar to that of normal TFBG without gold coating. For this temperature sensitivity characterization, the two ends of the TFBG-SPR sensor are fixed

#126816 - $15.00 USD Received 12 Apr 2010; revised 4 May 2010; accepted 4 May 2010; published 14 May 2010

by epoxy glue on a glass plate (to keep it perfectly straight) and placed in a distilled water bath provided with a temperature controller. In order to obtain precise temperature information in real time at the sensor location, a K-type thermocouple with a temperature resolution of 0.1 °C is placed in close proximity to the sensor in the water bath. The experiments were carried out over a temperature range of 23-59 °C in steps of 4 °C. Prior to the temperature characterization however, the refractive index sensitivity of the SPR sensor used must be calibrated at constant temperature. To determine the refractive index sensitivity of the TFBG-SPR sensor, we have measured its response at 23 °C by using a set of RI calibrated aqueous salt samples measured with an Abbe refractometer accurate to 1×10^{-4} RIU.

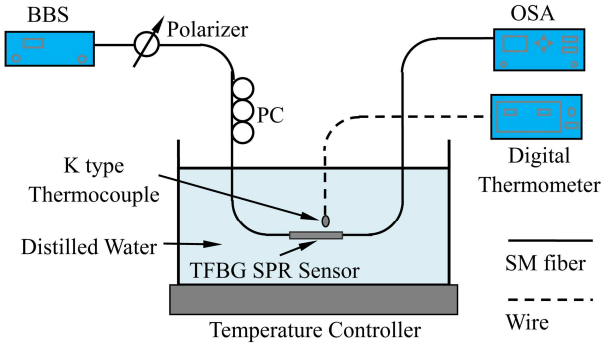

Fig. 2. Schematic diagram of the experimental setup for temperature calibration.

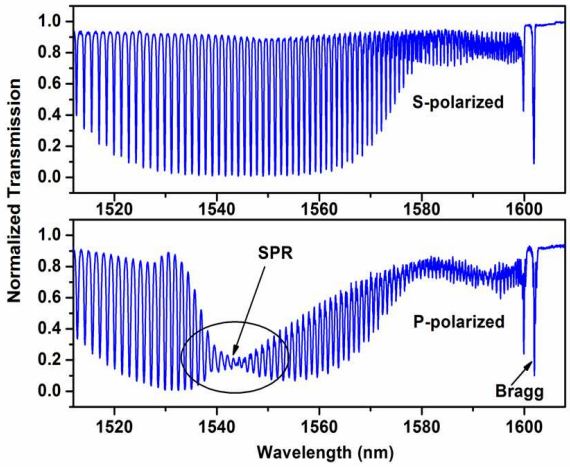

Fig. 3. Measured transmission spectrum of a TFBG-SPR sensor with a 50nm gold coating at two orthogonal linear polarization states (in distilled water).

3. Results and discussions

Before presenting the results, we use the self-referencing property of TFBG sensors to remove the contribution of the thermo-optic coefficients of the fiber grating from temperature dependence of the SPR. In short, this comes about because the Bragg wavelength and cladding mode resonance wavelengths λ_{Bragg} and λ_{clad}^{i} of TFBG are determined by the following phase matching condition [13]:

$$\lambda_{Bragg} = N_{eff}(core) * \Lambda / \cos(\theta), \qquad (1.a)$$

#126816 - $15.00 USD Received 12 Apr 2010; revised 4 May 2010; accepted 4 May 2010; published 14 May 2010

$$\lambda_{clad}^{i} = (N_{eff}(core) + N_{eff}^{i}(clad)) * \Lambda / \cos(\theta), \qquad (1.b)$$

where Λ is the grating period, θ the tilt angle of the grating fringes, $N_{eff}(core)$ and $N_{eff}^{i}(clad)$ are the effective index of the core mode and i th order cladding. But as temperature changes, all the cladding mode resonances of a bare TFBG shift by an amount equal to the shift of the core mode resonance, i.e.10 pm/°C [17]. Therefore if we offset the wavelength scale of all measured spectra so that their core mode resonance are lined up in wavelength, the remaining variations in the transmission spectra can only be due to changes in the gold coating and in the surrounding medium adjacent to the coating. In the present case, temperature changes will modify the refractive index of the water in which the fiber is immersed and the permittivity of the gold coating. Therefore the data analysis protocol proceeds as follows, using three of the spectra obtained in the course of our experiments as shown in Fig. 4.

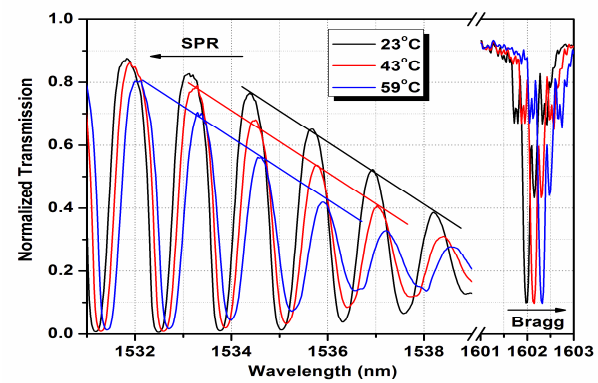

Fig. 4. Measured spectra of the TFBG-SPR sensor near the SPR resonance and near the Bragg wavelength, against temperature change in distilled water. The lines connecting the selected resonance peaks are used to calculate the SPR wavelength with the extrapolation method.

In each spectrum, the wavelength of the SPR is found by locating the most attenuated cladding mode resonances: these resonances correspond to modes that have become very lossy as a result of coupling to the surface plasmons [12]. It can be seen that the observed SPR resonance shift towards shorter wavelengths as the temperature increases from 23 °C to 59 °C. In practice we use the following method to pinpoint the shift of the SPR location between each spectrum: we fit four of the well defined resonances located on the edge of the SPR coupled region with a straight line and extrapolate this line up to the normalized background level which is 0.45 for the provided spectra (as shown in Fig. 4).The approach used here can be applied only if the spectra are not significantly deformed between experiments. The Bragg offset-corrected SPR shifts follow an approximately linear temperature dependence with a slope of –0.0686 nm/°C over this temperature range, where the *R*-squared value and rms deviation are 0.999 and 0.04, respectively. The results are to be presented graphically along with other results below.

However we will now proceed to demonstrate that much of this shift is due to the change in refractive index of the water. The RI of distilled water, as an empirical function of wavelength λ, temperature T, and density ρ, can be expressed by the following equation [18]:

$$\frac{n^2-1}{n^2+2}(1/\bar{\rho}) = a_0 + a_1\bar{\rho} + a_2\bar{T} + a_3\bar{\lambda}^2\bar{T} + a_4/\bar{\lambda}^2 + \frac{a_5}{\bar{\lambda}^2 - \bar{\lambda}_{UV}^2} + \frac{a_6}{\bar{\lambda}^2 - \bar{\lambda}_{IR}^2} + a_7\bar{\rho}^2, \quad (2)$$

where $\bar{\rho} = \rho/\rho^*$, $\bar{T} = T/T^*$, $\bar{\lambda} = \lambda/\lambda^*$; ρ^*, T^*, λ^*, a_0 - a_7, $\bar{\lambda}_{UV}$ and $\bar{\lambda}_{IR}$ are constants [18]. In the 1550 nm wavelength range, the refractive index of distilled water decreases

#126816 - $15.00 USD Received 12 Apr 2010; revised 4 May 2010; accepted 4 May 2010; published 14 May 2010

linearly from 1.3218 to 1.3167 with a slope rate of $-1.3*10^{-4}$ RIU/°C when the temperature rises from 23 °C to 59 °C.

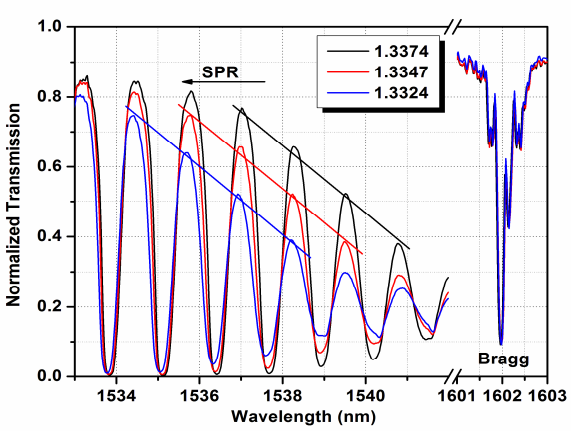

Fig. 5. Measured spectra of TFBG-SPR sensor against refractive index changes. The lines at selected resonance peaks are employed to calculate the SPR wavelength with the extrapolation method (similar to Fig. 4).

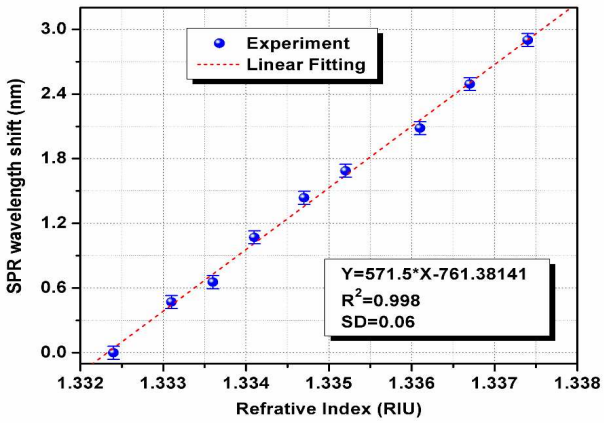

Fig. 6. SPR wavelength shifts against refractive index changes.

Figure 5 shows the measured spectra of the TFBG-SPR sensor against refractive index changes, where the RI values were calibrated by using an Abbe refractometer with a nominal accuracy of +/–0.0001. With the same approach of data analysis in Fig. 4, the SPR wavelength shifts against refractive index changes are illustrated in Fig. 6. Linear regression analysis yields a refractive index sensitivity of the SPR wavelength equal to + 571.5 nm/RIU (at 23 °C) with the R-squared value of 0.998. The rms deviation value (SD) between the linear fit and measured data is 0.06, which is equal to an uncertainty of 0.0001 RIU in the RI measurement by our TFBG SPR sensor (equal to the uncertainty of our calibration measurement using the Abbe refractometer). When the RI changes are very small, we also can measure the amplitude change of SPR resonance instead of its wavelength shift. As shown in ref. 12, the amplitude measurement of provides a higher sensitivity with a RI uncertainty of $4*10^{-5}$ RIU.

Using the linear regression calculated RI sensitivity (multiplied by the dn/dT value of water calculated above), we can add to Fig. 7 a data set representing the expected SPR shift due to the variation of the water RI with temperature (solid blue rectangles and linear fit). The difference between the measured SPR shift with temperature (circles) and expected shift from

#126816 - $15.00 USD Received 12 Apr 2010; revised 4 May 2010; accepted 4 May 2010; published 14 May 2010

the dn/dT of water (rectangles) represents the contribution of the sensor itself to the temperature dependence. The residual SPR wavelength temperature dependence (the upper data set shown in Fig. 7) has a fitted linear slope equal to + 6.3 pm/°C for the device configuration studied here.

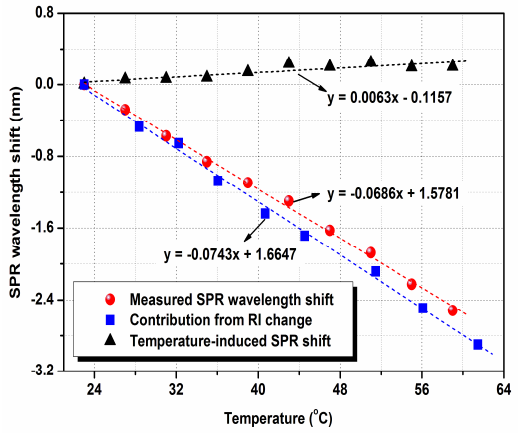

Fig. 7. SPR measured net wavelength shifts, shift from the RI change of water, and the difference between the two (due to the inherent temperature sensitivity of the sensor itself).

The SPR wavelength is uniquely determined by the permittivity of the gold layer and the refractive index of the outer medium. The residual temperature dependence of the SPR shift that we observe after taking into account the effect of temperature on the outer RI and also removing the effect of the thermo-optic coefficient of the FBG itself must be due to the thermo-optic effect of the gold film itself [14]. Here we present a theoretical calculation of this effect and compare it with our result. A surface plasmon with effective index N_{sp} can be expressed by the dielectric constant of the metal (ε_M) and the refractive index of surrounding measurand (n_s) according to the following condition [16]:

$$N_{sp} = \sqrt{\frac{\varepsilon_M n_s^2}{\varepsilon_M + n_s^2}}. \tag{3}$$

The dielectric function of gold layer is determined by using the modified Drude model [16]:

$$\varepsilon_M(\omega) = 1 - \frac{\omega_p^2}{\omega(\omega + i\omega_c)}, \tag{4}$$

where ω is the angular frequency of light, ω_c and ω_p are the collision frequency and plasma frequency, respectively. By using the same parameters as Ref. 16, the change of effective index N_{sp} with temperature is calculated to have a positive slope of $9.23*10^{-7}$/°C. At our operating wavelength of 1550 nm, the corresponding SPR wavelength shift induced by the permittivity change of the gold layer is thus + 0.51 pm/ °C, which is much smaller than our measurement result (+ 6.3 pm/ °C). The large difference between the two values is likely due to the underlying assumption we made that the thermal properties of the very thin gold film are the same as those of bulk gold material. In fact, it has already been shown that the complex refractive index of gold film is strongly dependent on the thickness (in the range of 16 nm to 70 nm) [19]. It is quite likely that the thermo-optic properties of the gold permittivity also depend strongly on thickness and hence on the residual shift. For the purpose of our sensor, this uncertainty on the residual shift can be lifted by proper calibration of the sensor

#126816 - $15.00 USD Received 12 Apr 2010; revised 4 May 2010; accepted 4 May 2010; published 14 May 2010

prior to use because the TFBG-SPR sensor has an internal thermometer provided by the absolute value of the Bragg wavelength of the core mode back reflection (completely insensitive to events surrounding the cladding). Measuring temperature at the same time as the SPR shift and using the calibrated residual temperature sensitivity of the sensor being used (+ 6.3pm/ °C here) allows temperature independent SPR shifts to be obtained. Obviously the RI of the material being measured also changes with temperature through its own thermo-optic coefficient but our calibrated sensor can provide an accurate RI reading for a material at the measurement temperature without contamination of the data by the temperature dependence of the sensor itself, a major issue in most SPR sensing schemes.

4. Conclusion

Using experimental results for the refractive index sensitivity of a single mode fiber TFBG-SPR sensor in water at different temperatures, and the self-referencing feature of the TFBG with temperature, we have demonstrated that the residual temperature dependence of the SPR shift measurement can be calibrated to + 6.3 pm/ °C at 1550nm in the temperature range from 23 °C to 59 °C. We further presented an elementary analysis of the origin of this residual sensitivity by calculating the temperature dependence of a "pure" plasmon at a single interface between gold and water. The experimental result differs from the theory by a factor of 12, likely because the thermo-optic properties of the very thin gold film used differ notably from those of bulk gold material. However, having provided a calibrated value for the residual temperature dependence of the SPR shift provides a way to remove this effect from any measurements since the core mode reflection wavelength of the TFBG can measure the temperature at the sensor location with great accuracy (typically 0.1°C), without influence from the outer medium refractive index. Therefore, we believe that a properly calibrated single mode fiber TFBG-SPR sensor can be used as an in situ biochemical sensor with truly temperature-independent results.

Acknowledgments

This work is partially supported by the Natural Sciences and Engineering Research Council of Canada, the Canada Foundation for Innovation, the Canada Research Chairs program, and LxDATA.

#126816 - $15.00 USD Received 12 Apr 2010; revised 4 May 2010; accepted 4 May 2010; published 14 May 2010